

Motional wave-packet splitting and ion-trap interferometry

Heping Zeng

Department of Physics, Faculty of Science, Kyoto University, Kyoto 606-01, Japan

(Received 1 May 1997)

For a single ion trapped in a harmonic potential under localization conditions beyond the Lamb-Dicke region, a motional wave packet can be coherently split by irradiating the trapped ion with appropriate counterpropagating traveling-wave laser pulses tuned to the second-sideband Raman resonance. Quantum interference between the split wave packets gives rise to interference fringes in the spatial probability distribution when the wave packets spatially overlap at a certain time during a periodic oscillation. An ion-trap interferometer is proposed on the basis of the wave-packet splitter in combination with quantum tomographic determination of the spatial interference fringes. [S1050-2947(97)07712-3]

PACS number(s): 32.80.Pj, 03.65.Bz, 42.50.Md, 42.50.Vk

In recent years, matter-wave interference with neutral atoms [1] has been demonstrated with material slits in Young's double-slit geometry [2], microfabricated gratings in a three-grating geometry [3], and mechanical effects of light fields on atomic beams [4]. In the latter context, coherent splitters of atomic beams, which are essential components of atomic interferometers, were realized by stimulated Raman transitions [5], adiabatic momentum transfer [6], and atomic wave diffraction using temporal slits [7]. Atomic interferences were also observed by nonadiabatic mixing of dressed states in a micromaser cavity [8].

In this paper, we propose to construct an interferometer with a single laser-cooled ion trapped in a harmonic potential. In principle, an ion-trap interferometer can be built by first splitting a single motional wave packet coherently, then propagating the split wave packets in different "paths," and finally spatially "recombining" the wave packets. It is interesting to note that any motional wave packets oscillate back and forth periodically in the harmonic trap. Two initially separated (but localized) motional wave packets will overlap at a certain time during an oscillatory period. If a quantum motional state, for example, the motional ground state (Gaussian-shaped wave packet) is coherently split into two symmetric vibrational wave packets localized at distinguishable positions, each of the split packets undergoes the same motion (but with a phase difference of π). The two resulting packets pass through and thus interfere with each other at the center point of the harmonic trap. Quantum interferences induce interference fringes in the spatial probability distribution, which are determined by the phase difference between the de Broglie waves associated with the two split wave packets. One can immediately see that the key step is to realize a coherent splitter of a motional wave packet.

Recently a mesoscopic superposition of spatially separated motional wave-packet states has been prepared with a single trapped ${}^9\text{Be}^+$ ion [9]. Appropriate sequential pulses of off-resonant laser beams were used to drive two-photon stimulated Raman transitions between the two internal hyperfine states of interest ${}^2S_{1/2}(F=2, m_F=-2)$ and ${}^2S_{1/2}(F=1, m_F=-1)$ (denoted by $|\uparrow\rangle$ and $|\downarrow\rangle$, respectively), or between different vibrational levels of the internal state $|\uparrow\rangle$. A typical experimental arrangement can be as follows. The trapped ion is initially prepared in the motional ground

state and a superposition of internal states $(|\uparrow\rangle + |\downarrow\rangle)/\sqrt{2}$. A pair of σ^- -polarized laser beams tuned to the first-sideband two-photon Raman resonance is applied to excite the motion correlated with the $|\uparrow\rangle$ component to a wave packet $|x_1\rangle$. After a Raman π -pulse excitation to flip the internal superposition, another first-sideband Raman excitation displaces the motional state correlated with the $|\uparrow\rangle$ component to a second wave packet $|x_2\rangle$. The internal and external (motional) states of the ion are then entangled. A final Raman $\pi/2$ -pulse excitation combines the two motional wave packets into two different motional superpositions correlated, respectively, with the two internal ground states $|\uparrow\rangle$ and $|\downarrow\rangle$

$$\Psi = \frac{|x_1\rangle - e^{i\delta}|x_2\rangle}{2} |\downarrow\rangle + \frac{|x_1\rangle + e^{i\delta}|x_2\rangle}{2i} |\uparrow\rangle, \quad (1)$$

where δ is associated with the related free time evolution of motion, and phase differences between the Raman beams. The features of the motional wave packets $|x_1\rangle$ and $|x_2\rangle$ are determined by the motional displacement driven by the two-photon Raman transitions between vibrational levels. In the Lamb-Dicke (LD) regime (or slightly beyond such a regime), both $|x_1\rangle$ and $|x_2\rangle$ approximate coherent wave-packet states. It is possible to set the two wave packets $|x_1\rangle$ and $|x_2\rangle$ to be localized at distinguishable positions with appropriate Raman displacements. On the other hand, if the trapped ion is far outside the LD regime, the two wave packet states $|x_1\rangle$ and $|x_2\rangle$ may have large spatial spreads and partly overlap each other in the position basis. As will be pointed out in what follows, the two wave packets usually become spatially indistinguishable. In such cases, we have to seek other ways to prepare a quantum superposition of spatially separated packets. It will be demonstrated in this paper that proper second-sideband Raman excitations may be used to split the motional ground state into two spatially separated wave packets.

Consider the interaction of a trapped ion with two off-resonant counterpropagating traveling-wave laser beams of frequencies ω_{L1} and ω_{L2} , respectively. We assume that the laser beams propagate along one of the principal axes of the trap potential, say, for example, the x axis. The two laser beams are tuned to the k th-sideband Raman resonance $\omega_{L1} - \omega_{L2} = k\nu$ ($k=1, 2, \dots$), where ν denotes the associ-

ated trap frequency along the x axis. The Raman interaction can be modeled by an effective Hamiltonian in the vibrational rotating-wave approximation [10]

$$\mathcal{H}_{k,\phi} = \hbar R e^{i\phi - \eta^2/2} f_k(a, a^\dagger) + \text{H.c.}, \quad (2)$$

where $f_k(a, a^\dagger) = \sum_{m=0}^{+\infty} (i\eta)^{2m+k} / [m!(m+k)!] a^{\dagger m} a^{m+k}$, R is the effective two-photon Raman coupling constant (real), η is the LD parameter, given by $\eta = |\Delta k_L|(\Delta x)_{gr}$, with $(\Delta x)_{gr}$ being the spatial spread of the vibrational ground state, ϕ and Δk_L are the phase and wave-number differences between the two applied laser beams, respectively, and $a = [m\nu/(2\hbar)]^{(1/2)} [x + ip/(m\nu)]$ is the usual annihilation operator for the harmonic oscillator (x and p are position and momentum operators, respectively, and m is the ionic mass). Note that we have worked in the weak Raman excitation region ($R \ll \nu$) and in the interaction frame rotating at the trap frequency ν .

We assume that the trapped ion is initially prepared in its vibrational ground state via laser-cooling techniques [11,12]. The Raman excitation drives the trapped ion to a motional state

$$|\psi_k\rangle_\phi = \exp[-i\vartheta(t)e^{i\phi - \eta^2/2} f_k(a, a^\dagger) + \text{H.c.}] |0\rangle, \quad (3)$$

where $\vartheta(t) = \int_0^t R(\tau) d\tau$ is the Raman pulse area. $|\psi_k\rangle_\phi$ can be numerically calculated by solving the Schrödinger equations with the Hamiltonian $\mathcal{H}_{k,\phi}$. For simplicity, we may assume that the free time evolution of a vibrational level $|n\rangle$ during the Raman interaction satisfies $e^{-i\nu t a^\dagger a} |n\rangle = |n\rangle$, i.e., $\nu t = 2m\pi$ ($m=1,2,\dots$). If $\nu t \neq 2m\pi$, one may let the ion evolve freely for an additional time t_1 till $\nu(t+t_1)/(2\pi)$ is an integer.

The above-mentioned motional wave packets $|x_1\rangle$ and $|x_2\rangle$ in Eq. (1) correspond to $|\psi_1\rangle_{\phi=0}$ and $|\psi_1\rangle_{\phi=\pi}$, respectively. In the LD limit, only the first-order terms of η in the above expression play a dominant role, and higher-order terms can be neglected in the spirit of the standard LD perturbation approximation. Therefore, $|\psi_1\rangle_{\phi=0}$ and $|\psi_1\rangle_{\phi=\pi}$ approximate coherent states $|\vartheta(t)\rangle$ and $|- \vartheta(t)\rangle$, respectively, where a coherent state $|\alpha\rangle$ is defined as usual $a|\alpha\rangle = \alpha|\alpha\rangle$. However, the Raman displacement will be nonlinearly modified when the LD parameter is relatively large. In Fig. 1, we compare the spatial probability distributions of the superposed motional wave packets $(|\psi_1\rangle_{\phi=0} + |\psi_1\rangle_{\phi=\pi})/2$ under different localization conditions. For large LD parameters, the two wave packets are spatially indistinguishable as shown in Fig. 1(b), and thus no longer suitable to construct an ion-trap interferometer. It is also clear that such a motional superposition is not a ‘‘Schrödinger cat’’ state [13].

Let us examine the nonlinearly modified second-sideband Raman excitations of the vibrational ground state. Figure 2 depicts the spatial probability distributions of the motional wave-packet $|\psi_2\rangle_{\phi=\pi/2}$. For a small LD parameter, the related effective Hamiltonian approximates $\mathcal{H}_{2,\phi} = -\hbar R \exp(i\phi) \eta^2 a^2/2 + \text{H.c.}$ (up to the second order of η), and therefore $|\psi_2\rangle_\phi$ is approximately a ‘‘vacuum-squeezed state’’, i.e., $|\psi_2\rangle_\phi = S(\epsilon)|0\rangle$, where $S(\epsilon) = \exp[(\epsilon a^{\dagger 2} - \epsilon^* a^2)/2]$ is the ‘‘squeeze’’ operator, with $\epsilon \equiv \exp(i\theta) = i\eta^2 \vartheta(t) \exp(-i\phi)$ [$r = \eta^2 \vartheta(t)$ is the squeezing parameter,

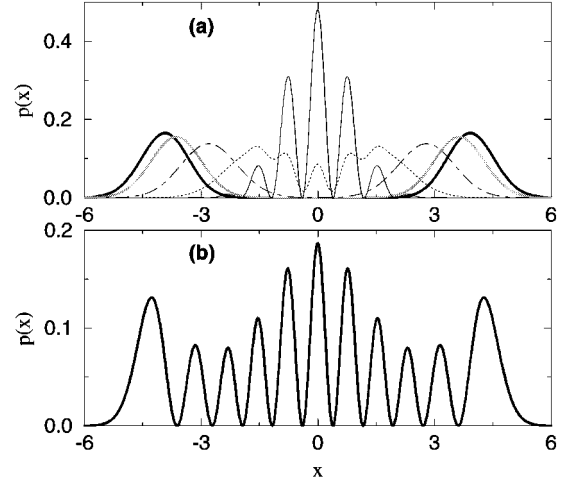


FIG. 1. The spatial probability distributions of the superposed motional wave packets $(|\psi_1\rangle_{\phi=0} + |\psi_1\rangle_{\phi=\pi})/2$, for $\vartheta(t)=15$ and $\eta=0.2$ (a) and $\eta=0.5$ (b), respectively. In (a), the associated free time evolution after preparation ($t_f=0$) is illustrated at time points $t_f=0$ (wide solid line), $t_f=T/16$ (grey line), $t_f=T/8$ (dot-dashed line), $t_f=3T/16$ (dotted line), and $t_f=T/4$ (solid line), respectively, where $T=2\pi/\nu$ is the oscillatory period. Figures 2 and 3 will use the same curve definition for the free time evolution.

and $\theta = \pi/2 - \phi$ is the squeezing angle]. For example, for a LD parameter $\eta=0.2$ and Raman pulse area $\vartheta(t)=50$, we can get a squeezed wave packet as shown in Fig. 2(a). In a recent experiment [14], a nearly ‘‘vacuum-squeezed’’ state has been attained with second-sideband Raman excitations. The vibrational occupational distribution was fitted as $p_{2n} = \text{sechr}(2n)! (\tanh r)^{2n} / (2^n n!)^2$, with $\beta \equiv \exp(2r) = 40 \pm 10$ [i.e., $\vartheta(t) = 45 \pm 3$]. On the other hand, a double-peaked spatial distribution can be attained with some larger Raman pulse areas. Figure 2(b) gives the spatial probability distribution for $\vartheta(t)=80$. We note that a ‘‘vacuum-squeezed’’ state $|\psi_{sq}\rangle = S(r)|0\rangle$ can be expressed in the position representation as $\langle q|\psi_{sq}\rangle = \psi(q, \sigma_q) = [1/(\pi\sigma_q^2)]^{1/4} \exp(-q^2/2\sigma_q^2)$ with $\sigma_q = \exp(-r)$ and $q = (a + a^\dagger)/\sqrt{2}$. Hence, a double-peaked wave packet differs from a ‘‘vacuum-squeezed’’

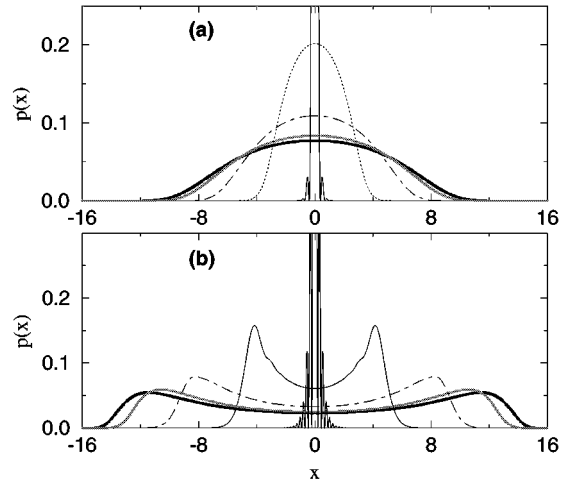


FIG. 2. The spatial probability distributions of $|\psi_2\rangle_{\phi=\pi/2}$ and the associated free evolutions for $\eta=0.2$ and $\vartheta(t)=50$ (a) and $\vartheta(t)=80$ (b), respectively.

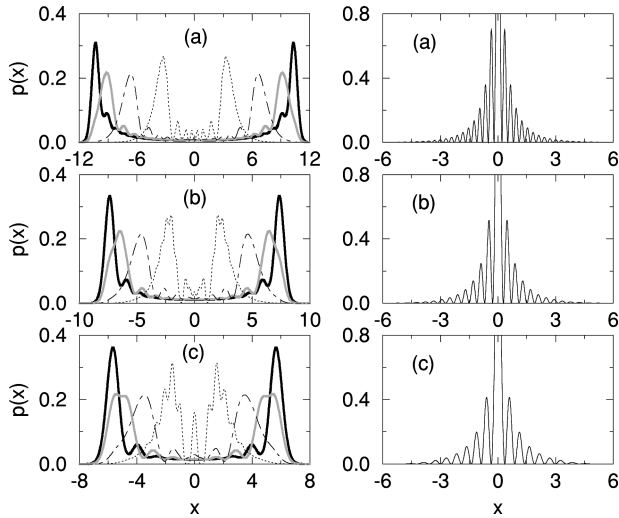


FIG. 3. The spatial probability distributions of $|\psi_2\rangle_{\phi=\pi/2}$ and the associated free time evolution for $\eta=0.3$ and $\vartheta(t)=50$ (a), $\eta=0.4$ and $\vartheta(t)=25$ (b), and $\eta=0.5$ and $\vartheta(t)=15$ (c), respectively. For clarity, each of parts (a), (b), and (c) is split into two graphs, respectively.

state (Gaussian-shaped). The difference originates in the nonlinear modification of the associated second-sideband vibronic coupling constants between vibrational levels $|n\rangle$ and $|n+2\rangle$, which are proportional to

$$\begin{aligned} |\Omega_{n,n+2}| &= |\langle n | \exp[i\eta(a+a^\dagger)] | n+2 \rangle| \\ &= \frac{1}{2} \eta^2 \sqrt{(n+1)(n+2)} + O(\eta^4) \end{aligned}$$

When n is large and η is not too small (for example, $\eta=0.2$), the nonlinear terms included in $O(\eta^4)$ produce significant effects on the Raman excitation. For larger LD parameters, the nonlinearly modified second-sideband Raman excitations with appropriate areas $\vartheta(t)$ can even split the motional ground state into two spatially separated wave packets. In Fig. 3, we plot the spatial probability distributions of the wave packets for LD parameters and Raman pulse areas $\eta=0.3$ and $\vartheta(t)=50$ (a), $\eta=0.4$ and $\vartheta(t)=25$ (b), and $\eta=0.5$ and $\vartheta(t)=15$ (c), respectively. Numerical calculations show that there exists a particular range of $\vartheta(t)$ with which the second-sideband Raman excitations are approximately equivalent to a coherent splitter of the motional ground (Gaussian-shaped) wave packet. For example, Fig. 4 indicates that spatial splittings can be attained with $\vartheta(t)=15\text{--}30$ and $\eta=0.4$. Such coherent splitters of motional wave packets (and the associated de Broglie waves) are analogous to light beam splitters. Physically, the splitting originates in the quantum interference between vibrational levels. If the motional state is prepared in a proper superposition of vibrational Fock states, there may exist destructive interferences in a wide range around the center point of the trap, leading to a vanishing local spatial probability. Therefore the resulting wave packet consists of two spatially separated parts. The free time evolution of the motional states changes the relative phase angles of the vibrational Fock-state components, and thus changes the interference features. When the two parts spatially overlap at the center of the trap

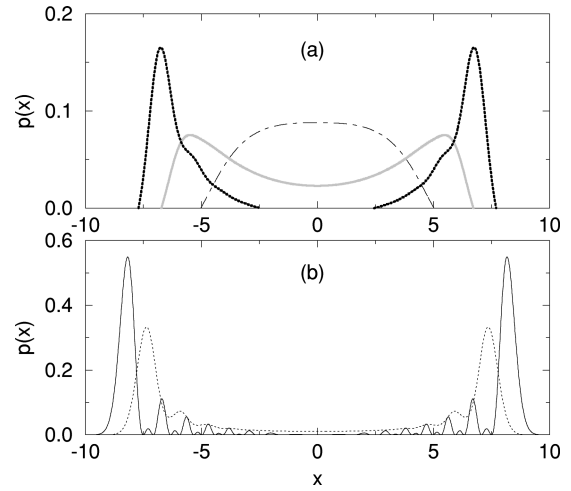


FIG. 4. The spatial probability distributions of $|\psi_2\rangle_{\phi=\pi/2}$ at $t_f=0$ for $\eta=0.4$. The Raman pulse area is selected as $\vartheta(t)=10$ (dot-dashed line), 15 (grey line), 20 (wide dotted line), 25 (dotted line), and 30 (solid line), respectively. For clarity, the graph is split into two parts, (a) and (b).

during the oscillation, interference fringes can be expected in the spatial probability distribution.

Consequently, one may build an ion-trap interferometer in the following steps. (i) Cool the trapped ion to the vibrational ground state by the sideband [12] or stimulated Raman sideband laser-cooling scheme [11]. In order to be effectively cooled to the zero point of motion, the ion should be tightly confined [15]. With the use of resolved-sideband stimulated Raman cooling, a pure quantum-mechanical ground state of motion was recently attained with a probability of 98% [11]. (ii) Adiabatically reduce the trap frequency so that a relatively large LD parameter can be obtained. For example, one may double the LD parameter by decreasing the value of the trap frequency to its quarter. Because the trap frequency is changed adiabatically, the trapped ion will remain in the vibrational ground state with unchanged occupation probability [16]. This step may be unnecessary if one already has a relatively large LD parameter, say, for example, $\eta=0.4$ or larger. (iii) Apply a second-sideband Raman excitation to excite the vibrational ground state. An appropriate Raman pulse area should be selected so that one can achieve a coherent superposition of spatially separated motional wave packets; i.e., the second-sideband Raman interaction is tailored as a coherent splitter of the motional wave packets. (iv) Wait for a certain time while the trapped ion evolves freely in the trap till the split wave packets spatially overlap. A quantum-tomographic measurement [17–20] is then applied. Many proposals have been suggested to reconstruct motional states of a trapped ion [21–23]. More recently, the density matrices of various quantum motional states have been determined by applying different coherent displacements and measuring number state populations [24]. The spatial interference fringes can be observed by such a tomographic measurement [25].

In summary, we have demonstrated that an appropriate second-sideband Raman excitation of the motional ground state can be used to prepare a quantum superposition of two spatially separated wave packets. The splitting of the Gaussian-shaped motional wave packet (ground state) is in-

trinsically straightforward. We note that an indirect splitter of the motional ground state wave packet was recently realized by “combining” different motional wave packets correlated with different internal state components with the use of Raman pulse sequences [9]. Unfortunately, this scheme becomes invalid for trapped ions with relatively large LD parameters. We emphasize that the second-sideband Raman excitation scheme is particularly suitable for trapped ions beyond the LD regime. It can be employed for any internal ground state. It is possible to prepare separated motional wave packets with all the population in only one internal level. An ion-trap interferometer is then proposed operating on coherent motional wave-packets splitting and “recombining.” Using a strong excitation and adiabatic passage to split the vibrational wave packet, Poyatos *et al.* [26] recently proposed a different ion-trap interferometer. Experiments suggested in this paper simply make the use of appropriate

second-sideband excitations that require only single laser pulses. The spatial interference fringes in an ion-trap interferometer are sensitive to the vibrational coherence. Note that environment-system couplings continuously decohere vibrational superpositions into statistical mixtures [27]. An ion-trap interferometer may be useful to study quantum decoherences [28], in particular to study deliberate decoherences induced by coupling the motional superpositions to an “engineered” reservoir [29].

The author thanks Professor Herbert Walther for his hospitality at Max-Planck-Institute of Quantum Optics, and Professor T. Yabuzaki for his hospitality at Kyoto University. The author is grateful for the financial support from the Max-Planck Society and from Japan Society for the Promotion of Science. Valuable discussions with A. Baldauf, H. Kakori, W. Lange, and S. Schlipf are acknowledged.

-
- [1] See, for example, *Atom Interferometer*, edited by Paul R. Berman (Academic Press, New York, 1997), and references therein.
- [2] O. Carnal and J. Mlynek, *Phys. Rev. Lett.* **66**, 2689 (1991).
- [3] D. W. Keith, C. R. Ekstrom, Q. A. Turchette, and D. E. Pritchard, *Phys. Rev. Lett.* **66**, 2693 (1991).
- [4] See, for example, articles in *Appl. Phys. B* **54** (1992).
- [5] M. Kasevich and S. Chu, *Phys. Rev. Lett.* **67**, 181 (1991); D. S. Weiss, B. C. Young, and S. Chu, *ibid.* **70**, 2706 (1993).
- [6] P. Marte, P. Zoller, and J. L. Hall, *Phys. Rev. A* **44**, R4118 (1991); J. Lawall and M. Prentiss, *Phys. Rev. Lett.* **72**, 993 (1994); L. Goldner *et al.*, *ibid.* **72**, 997 (1994).
- [7] P. Szriftgiser, D. Guery-Odelin, M. Arndt, and J. Dalibard, *Phys. Rev. Lett.* **77**, 4 (1996).
- [8] G. Raithel, O. Benson, and H. Walther, *Phys. Rev. Lett.* **75**, 3446 (1995).
- [9] C. Monroe, D. M. Meekhof, B. E. King, and D. J. Wineland, *Science* **272**, 1131 (1996).
- [10] W. Vogel and R. L. de Matos Filho, *Phys. Rev. A* **52**, 4214 (1995).
- [11] C. Monroe, D. M. Meekhof, B. E. King, S. R. Jefferts, W. M. Itano, and D. J. Wineland, *Phys. Rev. Lett.* **75**, 4011 (1995).
- [12] F. Diedrich, J. C. Bergquist, W. M. Itano, and D. J. Wineland, *Phys. Rev. Lett.* **62**, 403 (1989).
- [13] E. Schrödinger, *Naturwissenschaften* **23**, 807 (1935); **23**, 823 (1935); **23**, 844 (1935).
- [14] D. M. Meekhof, C. Monroe, B. E. King, W. M. Itano, and D. J. Wineland, *Phys. Rev. Lett.* **76**, 1796 (1996).
- [15] S. R. Jefferts, C. Monroe, E. W. Bell, and D. J. Wineland, *Phys. Rev. A* **51**, 3112 (1995).
- [16] J. Chen *et al.*, *Phys. Rev. Lett.* **69**, 1344 (1992); A. Kastberg *et al.*, *ibid.* **74**, 1542 (1995).
- [17] D. T. Smithey, M. Beck, M. G. Raymer, and A. Faridani, *Phys. Rev. Lett.* **70**, 1244 (1993); for the theory, see K. Vogel and H. Risken, *Phys. Rev. A* **40**, 2847 (1989).
- [18] T. J. Dunn, I. A. Walmsley, and S. Mukamel, *Phys. Rev. Lett.* **74**, 884 (1995).
- [19] W. Vogel *et al.*, *J. Opt. Soc. Am. B* **4**, 1633 (1987).
- [20] P. J. Bardroff *et al.*, *Phys. Rev. A* **51**, 4963 (1995); **53**, 2736 (1996).
- [21] S. Wallentowitz and W. Vogel, *Phys. Rev. Lett.* **75**, 2932 (1995).
- [22] J. F. Poyatos, R. Walser, J. I. Cirac, P. Zoller, and R. Blatt, *Phys. Rev. A* **53**, R1966 (1996).
- [23] P. J. Bardroff, C. Leichtle, G. Schrade, and W. P. Schleich, *Phys. Rev. Lett.* **77**, 2198 (1996).
- [24] D. Leibfried, D. M. Meekhof, B. E. King, C. Monroe, W. M. Itano, and D. J. Wineland, *Phys. Rev. Lett.* **77**, 4281 (1996).
- [25] U. Leonhardt and M. G. Raymer, *Phys. Rev. Lett.* **76**, 1985 (1996); T. Richter and A. Wünsche, *Phys. Rev. A* **53**, R1974 (1996).
- [26] J. F. Poyatos, J. I. Cirac, R. Blatt, and P. Zoller, *Phys. Rev. A* **54**, 1532 (1996).
- [27] W. H. Zurek, *Phys. Today* **44**(10), 36 (1991).
- [28] D. P. DiVincenzo, *Science* **270**, 255 (1995); J. I. Cirac, T. Pellizzari, and P. Zoller, *ibid.* **273**, 1207 (1996).
- [29] J. F. Poyatos, J. I. Cirac, and P. Zoller, *Phys. Rev. Lett.* **77**, 4728 (1996).